

This is a post-print version of Col. Surf. B: Biointerfaces Vol. 88 (2), 1 December 2011, pp. 601–609

Protein delivery based on uncoated and chitosan-coated mesoporous silicon microparticles

Ester Pastor¹, Eugenia Matveeva¹, Angela Valle-Gallego², Francisco M Goycoolea², and Marcos Garcia-Fuentes^{2*}

¹ EM-Silicon Nanotechnologies S.L., Parque Científico de la Universidad de Valencia, C/ Catedrático Agustín Escardino, 9. 46980 Paterna (Valencia), Spain.

² NANOBIOFAR Group, Department of Pharmacy and Pharmaceutical Technology, University of Santiago de Compostela, 15782, Santiago de Compostela, Spain.

* To whom correspondence should be addressed:

Marcos Garcia Fuentes, Ph.D.

Dep. de Farmacia y Tecnología Farmacéutica, Facultad de Farmacia

Universidad de Santiago de Compostela, Campus Vida

15782 Santiago de Compostela, Spain

TLF: +34881814887

FAX: +34981547148

E-MAIL: marcos.garcia@usc.es

Abstract

Mesoporous silicon is a biocompatible, biodegradable material that is receiving increased attention for pharmaceutical applications due to its extensive specific surface. This feature enables to load a variety of drugs in mesoporous silicon devices by simple adsorption-based procedures. In this work, we have addressed the fabrication and characterization of two new mesoporous silicon devices prepared by electrochemistry and intended for protein delivery, namely: (i) mesoporous silicon microparticles and (ii) chitosan-coated mesoporous silicon microparticles. Both carriers were investigated for their capacity to load a therapeutic protein (insulin) and a model antigen (bovine serum albumin) by adsorption. Our results show that mesoporous silicon microparticles prepared by electrochemical methods present moderate affinity for insulin and high affinity for albumin. However, mesoporous silicon presents an extensive capacity to load both proteins, leading to systems where protein could represent the major mass fraction of the formulation. The possibility to form a chitosan coating on the microparticles surface was confirmed both qualitatively by atomic force microscopy and quantitatively by a colorimetric method. Mesoporous silicon microparticles with mean pore size of 35 nm released the loaded insulin quickly, but not instantaneously. This profile could be slowed to a certain extent by the chitosan coating modification. With their high protein loading, their capacity to provide a controlled release of insulin over a period of 60-90 min, and the potential mucoadhesive effect of the chitosan coating, these composite devices comprise several features that render them interesting candidates as transmucosal protein delivery systems.

Keywords: porous silicon, electrochemical pore formation, chitosan, insulin, BSA, proteins, controlled drug delivery.

Introduction

Since the first works on the controlled delivery of biopharmaceutics, intensive research has focused on the design of new compositions capable of ensuring optimal encapsulation and release of these delicate and complex drugs. The use of composite nanostructured materials in pharmaceutical technology is a powerful approach that opens new possibilities for the development of highly functional drug delivery devices. Better known in microelectronics, nanostructured semiconductors have been recently recognized to bear great promise for biomedical purposes such as tissue engineering [1], medical diagnosis [2], and drug delivery [3, 4]. One of the most interesting features of porous silicon is its long-term stability at low pH (<6.0) [5] and the high hydrophobic nature of its native surface that can be extremely advantageous for the adsorption and delivery of small hydrophobic molecules such as doxorubicin [6], dexamethasone [7] or porphyrins [8]. Although the biocompatibility status of mesoporous silicon is still under investigation, it is known that the bulk material has negligible cytotoxicity [9]. Similar positive results have been observed for mesoporous silicon microparticles particles with sizes above 10 μm [10]. Mesoporous silicon is also biodegradable, and the kinetics of this process can be tailored both by modulating particles and size and by modifying the chemistry of its surface [11]. Overall, mesoporous silicon is attracting interest in the pharmaceutical field and several recent reviews have addressed its potential for controlled release devices [12, 13].

The most distinctive property of mesoporous silicon is its extremely large specific surface area arising from its complex nanostructure. This specific surface area is commonly greater than 300 m^2/g , and hence, it allows loading many kinds of drugs by simple adsorption. Adsorption-based loading procedures can be optimal for protein formulation, considering that the delicate tertiary structure of these molecules should be preserved to maintain their bioactivity. Mesoporous silicon structure and chemistry (i.e. pore diameter, surface chemical terminations) can be easily tailored leading to controlled dissolution rates under physiological conditions. By careful fine-tuning the porous silicon carrier properties it is possible

to attain zero order drug release kinetics and develop novel pharmaceutical devices such as insulin pumps [14,15] and gastrointestinal patches for oral insulin delivery [16,17]. Some recent studies have studied protein loading into porous silicon layers [18-21], and there is a general consensus that this is a complex process that can be influenced by the morphology of the silicon device, its nanostructure, and the device surface chemistry [22]. However a systematic approach would improve our understanding of the physicochemical processes involved in protein-porous silicon interaction, and ultimately, it would lead to optimized formulations for protein delivery.

For mesoporous silicon systems intended for transmucosal drug delivery, a suitable particle size might be 10-30 μm , since they combine low toxicity with high available surface area for potential interaction with biological mucosae [10]. In this work, we have studied thermoxidized mesoporous silicon prepared by an electrochemical method in the form of microparticles (MS-MPs) as potential drug delivery devices for a therapeutic protein (insulin) and a model antigen (bovine serum albumin, BSA). These two proteins present very different physicochemical properties, making them suitable models to perform comprehensive studies characterizing protein adsorption on MS-MPs. At a subsequent stage, MS-MPs were modified through the deposition of a chitosan (CS) coating, thus forming a multifunctional silicon/polymer composite with potential for advanced biomedical applications, a concept that has been recently explored in some recent works [23, 24]. The rationale behind the selection of CS as the coating polymer was: (i) its known capacity to adsorb to polyactionic surfaces, (ii) its established pharmaceutical record, (iii) and its mucoadhesiveness and permeation enhancing properties [25-28]. The global concept was to generate a drug delivery system that would combine silicon drug loading properties with the unique characteristics of CS-coated systems for transmucosal drug delivery. The final composite system should also provide adequate release kinetics and be presented in an easily administered form.

Experimental Details

In the supplementary material (Figure S1) we illustrate the step-by-step procedure followed for the preparation of the different MS-MPs formulations.

Materials. The following chemicals were obtained from commercial sources and used as received. Silicon from Si Materials from Germany, boron doped with a resistivity of 0.01-0.02 Ohm·cm (p+); wafer diameter was 100.0 ± 0.5 mm and thickness of 525 ± 25 mm (isoelectric point (pI) = $\sim 2 - 3.5$). HF (48%) from Riedel de Haën (Germany) and ethanol (96%) from Panreac (Spain). Synthetic air (N₂ with 21 % of O₂) was provided from Abello Linde S.A (Spain). Insulin human (recombinant expressed in yeast, 28.7 IU mg⁻¹, pI= ~ 5.3) and Albumin (from bovine serum, BSA, pI= ~ 4.9) were acquired from Sigma Aldrich. Acetic acid and sodium acetate anhydride and phosphate buffer saline (PBS) were acquired from Sigma Aldrich. Four different CS samples were employed in this work. They were purified from a batch of squid pen CS (from Mathani, France). Their M_w, expressed as degree of polymerization (DP), low (LDP) or high (HDP), and the degree of acetylation (DA, %) were characterized by HPLC-MALLS-DRI and ¹H NMR spectroscopy, respectively, as described elsewhere [29]. These four CS samples were: (i) HDP (266000 g/mol)-DA 56, pK_a=6.80; (ii) HDP (124000 g/mol) -DA 1 pK_a=6.46, (iii) LDP (13200 g/mol) -DA 1- pK_a=6.46 and (iv) LDP (11420g/mol)-DA 51, pK_a=6.74. CS was dissolved in 5% stoichiometric excess of acetic acid in aqueous solution. All other reagents were of analytical grade. Milli-Q water was used throughout the study.

Preparation of mesoporous silicon microparticles (MS-MPs). Porous silicon layers were prepared through an electrochemical treatment of the p+ silicon wafer (with 4 inches of diameter) in fluoric acid (48%): ethanol (96%) 1:2 electrolyte under 50 mA/cm² of current density. During the electrochemical treatments, the front side of the wafer was exposed to the electrolyte. After 1 hour of anodizing, the

thickness of the porous layer was approximately 300 μm . The silicon wafer was then washed throughout with distilled water and the porous fraction scratched from the remnant silicon wafer. To stabilize this mesoporous silicon layer a thermal oxidation process was performed under a synthetic air atmosphere at 450°C for one hour (Ivoclar-Vivadent Technical Owen, Programat P200 equipped with a vacuum pump VP3 and gas inlet). To reduce the particle size to the micrometer scale, the mesoporous silicon layer was milled and sieved in cascade. The fraction between 30 and 100 μm was selected for further studies. Henceforth this fraction is referred to as mesoporous silicon microparticles (MS-MPs).

Physicochemical characterization of the MS-MPs. The porosity of the porous silicon materials was determined gravimetrically by comparing the mass of the initial wafer, the mass of the silicon wafer after anodization, and the mass of the remaining wafer after removing the porous layer by scratching and after cleaning the remaining wafer with KOH 1M. The equation used is presented in the supplementary material (Equation 1).

The chemical composition of mesoporous silicon layer was analyzed by Fourier Transformed Infrared (FTIR). Spectra were acquired on a Perkin-Elmer Spectrometer (System 2000 FTIR) using the diffuse reflectance accessory. The chemical composition of MS-MPs was analyzed using Photoelectron Spectroscopy (XPS) analysis (Thermo Scientific K-Alpha Instrument, Thermo Fisher Scientific, equipped with a monochromatic Al α (1486.6eV) X-ray source).

To determine the particle size distribution of MS-MPs, samples were analysed by an optical microscope (Olympus BX60) equipped with a video camera and linked to a computer with an image analyzing software (VGA 24 Analyser Software). Pictures were first digitalized with a Matrox Comet video card (Matrox Electronic Systems). Particle size distribution was found to be log-normal ($r^2 > 0.99$) and average particle size and standard deviation was calculated after fitting particle distribution to this model. The morphology of unloaded or protein-loaded MS-MPs was visualized by high resolution Scanning Electron Microscopy (SEM, Hitachi S4500). Additionally, the BET surface area of the MS-

MPs sample was determined by N₂ adsorption-desorption isotherms (Micrometrics ASAP 2020 V3.04H, Micromeritics France S.A., France).

Protein-loading of MS-MPs. The capacity of MS-MPs to load proteins by adsorption was studied as a function of several variables: protein nature (i.e. insulin vs. BSA), protein concentration (0.1-3.5 mg/ml for insulin; 0.1-25 mg/ml for BSA) and pH (pH 3.8 and 7.4, i.e. opposite protein net charge). For protein adsorption, 1 ml of insulin or BSA were incubated in acetate (pH 3.8) or phosphate buffer (pH 7.4) with a fixed amount of MS-MPs (2 mg) during 30 min, and under horizontal shaking (90-95 rpm, Heidolph Promax 2020, Germany) at 37°C.

Determination of protein Association Efficiency and MS-MPs Loading Capacity. The amount of protein loaded into MS-MPs was calculated indirectly from the difference between the total amount of protein used for adsorption and the protein equilibrium concentration after adsorption (i.e. free protein concentration in the supernatant). The protein equilibrium concentration was determined following isolation of the protein solution from the microparticles suspension by centrifugation (12800 x g during 10 min at 37°C). The supernatant was diluted with phosphate buffer 7.4 and assayed for protein content by the Lowry method (Micro BCA Protein Assay Reagent Kit, Pierce, USA) using a UV-1603 Shimadzu (Japan) spectrophotometer set at 562 nm. Firstly, curves showing protein mass adsorbed vs. equilibrium concentration were plotted. Secondly, two pharmaceutically relevant parameters were calculated: the protein Association Efficiency (AE) and the MS-MPs Loading Capacity (LC). Protein AE represents the percentage of protein associated to MS-MPs in relation to the total amount of protein. MP-MPs LC represents the percentage represented by the associated protein mass in relation to the total formulation. See detailed equations in the supplementary information (Equations 2 and 3).

Preparation and characterization of CS-coated MS-MPs. Both, unloaded and protein-loaded MS-MPs were coated with CS solutions at several concentrations (from 0.2 to 2 mg/ml). Briefly, 1 ml of CS solution were diluted in acetate buffer (pH 3.8) and incubated with 2 mg of isolated MS-MPs for 1h under horizontal shaking (~90-95 rpm) at 37°C. The amount of CS adsorbed was determined indirectly

by measuring the concentration of non-attached CS after isolation of the free CS solution from the MS-MPs (12800 x g during 10 min at 37°C). CS concentration was determined through a colorimetric test based in the reaction of CS with Cibacron brilliant red 3B-A [30]. The influence of CS physicochemical parameters on its capacity to associate to MS-MPs was studied.

Atomic Force Microscopy (AFM) was used to observe the surface of the CS coated samples (unloaded and protein-loaded). AFM was performed in air using the NanoScope III by Digital Instruments operating in tapping mode. Nanoscope 4.43r8 software was used for data analysis.

In vitro protein release study. Insulin release was studied in vitro by incubating aliquots of insulin-loaded MS-MPs in acetate (pH 5.5) or phosphate buffer (pH 7.4) under horizontal shaking (~90-95 rpm) at 37°C. Both CS-coated and uncoated formulations were tested, and the MS-MPs mass was adjusted to perform the experiment under sink conditions. At pre-established time intervals (5, 45, 60, 90, 130 and 150 min) aliquots from the release media were taken. Insulin solutions were isolated from microparticles by centrifugation (12800 x g during 10 min at 37°C). Protein concentration was determined by a Lowry assay as previously described. Insulin release is expressed as percentage of the total insulin loaded in the MS-MPs.

Result and Discussion

In this work we have studied mesoporous silicon microparticles (MS-MPs) prepared by a new electrochemical method as drug delivery devices for a therapeutic protein (insulin) and a model antigen (BSA). Firstly, we studied the physico-chemical properties of unloaded MS-MPs, including chemical composition, nanostructure and porosity. In a second stage, we systematically characterized the capacity of these compositions to load these proteins, providing further mechanistic insight on protein-mesoporous silicon interaction. Finally, unloaded and protein loaded MS-MPs were modified with

chitosan (CS) coating. The capacity of uncoated and CS-coated MS-MPs to release insulin was studied. The overall experimental approach is depicted in the supplementary material (Figure S1).

Preparation and characterization of porous silicon carriers. A porous silicon layer was prepared electrochemically and surface-modified afterwards by thermal oxidation as described in the methods section. Silicon oxidation is a superficial chemical treatment performed (i) to reduce the hydrophobicity of the starting material, (ii) to increase its chemical stability in aqueous solvents [31-32] and (iii) to control silicon-protein interactions [33]. Chemical analysis of the mesoporous silicon wafer used for microparticles preparation is shown in Figure 1. An FTIR spectrum of the Si-H_x vibration region of the native silicon layer before and after the oxidative treatment is shown in Figure 1A. The 2300-2150 cm⁻¹ vibration bands correspond to the native Si-H groups, whereas the 2150-2000 cm⁻¹ bands are assigned to back-bonded O-Si-H_x species –i.e. chemical species formed at the first stage of porous silicon oxidation (see Bisi et al. for further information on spectrum assignment [34]). This type of oxide arises from the incorporation of O atoms between the two most superficial silicon (Si) atoms that still hold native hydrogen (H) atoms. Other vibrations like Si-O-Si (~1100 cm⁻¹) or Si-OH (~3400 cm⁻¹) have also been found in oxidized material (spectral region not shown). Chemical analysis of the porous silicon wafer surface was performed by XPS. The results confirmed that oxygen was incorporated on the surface of the porous layer (40 ±4 %) during the thermal oxidation process (Figure 1B). This study also showed the presence of residual carbon (app. 4 ±2 %), presumably arising from the ethanol used as an electrolyte component in the anodizing procedure. In summary, compared to traditional supramolecular chemistry approaches that lead to uniform SiO₂ structures, MS-MPs prepared by electrochemistry result in a pure Si matrix, and a Si-H_x surface. This surface can be oxidized to obtain Si oxide outer layers that are more stable in biological fluids.

MS-MPs were prepared by dry milling of the oxidized mesoporous silicon layer, and therefore they represent an industry-friendly top-down alternative to the more classical bottom-up supramolecular

synthesis strategies. SEM images confirmed the formation of particles with a log-normal particle sized distribution. Average particle size was 33.1 μm , and standard deviation 27.3 μm (Figure 2A). Figure 2B illustrates the resulting particle size expressed as a volume fraction distribution. The presence of a minor fraction (6-8% of the particles in volume distribution) with sizes larger than 80 μm can be associated with agglomeration or irregular shape. This fraction of aggregated particles is relatively small as we take it from a particle number percentage rather than by volume distribution. The inner structure of MS-MPs was characterized by SEM imaging (2C, 2D) and N_2 adsorption/desorption isotherms (2E, isotherms; 2F, surface area/pore volume). MS-MPs are characterized by an average pore diameter of 22.5 nm (N_2 adsorption, BJH calculation scheme) and a BET Surface Area of 341.5219 m^2/g . It is known that porous silicon prepared with p⁺-type doped wafer consists on long tubular cavities running perpendicular to the surface, another distinctive feature of MS-MPs as compared to silicon particles prepared by supramolecular chemistry [34]. Figure 2C and 2D substantiate the order of magnitude of this pore size and this regular pore arrangement. The porosity of the material was 83 \pm 4 %, as determined gravimetrically.

Protein loading. Considering the outstanding specific surface of MS-MPs (\sim 340 m^2/g), we hypothesized that these nanostructured systems could be highly suitable for loading biopharmaceuticals by adsorption. Adsorption of biopharmaceuticals from aqueous solutions is an ideal method for drug loading since it does not require high mechanical energy, use of organic solvents or high temperatures, factors that might lead to the denaturation or chemical degradation of protein drugs. In this work, we have studied the capacity of MS-MPs to load two different proteins by adsorption, namely insulin and BSA. In Figure 3A the adsorption isotherms of insulin onto MS-MPs are presented at two pH values. The corresponding BSA adsorption isotherms are shown in Figure 3B. In all experiments, protein concentrations in the protein solution were always below their solubility limit, which was only limiting for insulin at pH 7.4 (4-4.5 mg/ml).

Insulin adsorption isotherms were linear at both pH values, indicating that no saturation point in the adsorption process is achieved with the highest equilibrium concentration tested. Acidic media (pH 3.8) favored insulin adsorption as the slope between amount of insulin adsorbed and equilibrium concentration almost doubled as compared to that at pH 7.4. In the case of the BSA isotherms at pH 3.8, a saturation point is clearly reached for concentrations above 0.3 mg/ml. At pH 7.4, BSA adsorption on MS-MPs did not reach any limit value even at extreme equilibrium concentration values (3.5 mg of BSA/mg of MS-MPs). The markedly different affinity of BSA for MS-MPs at different pH values might be caused by a different hydrophobic/hydrophilic balance of BSA at these two pH values.

Figure 4 summarize the most relevant pharmaceutical parameters describing protein association to MS-MPs. The association efficiency (AE) describes the percentage of total protein that associates to the carrier. The loading capacity (LC) shows the percentage of the final formulation mass represented by the loaded protein. For insulin, AE reached a 60% limit at the lowest protein concentration tested (Figure 4A). This value was approximately maintained through all the studied concentration range. At low insulin concentrations, some differences on protein adsorption were observed at pH values of 3.8 and 7.4. The AE of insulin at pH 3.8 was always close to the maximum value. At pH 7.4, insulin AE increased linearly between 0 and 0.6 mg/mL of insulin concentration and then reached a stable maximum. In both cases, the insulin LC in MS-MPs increased in a linear fashion over the studied concentration range (Figure 4C). Under the current experimental setup we reached LC values around 50%, i.e. an equivalent mass of silicon and proteins loaded in the formulation.

The association of BSA follows a different behaviour than insulin at low pH. In this case, the AE of BSA to MS-MPs is very high at low protein concentrations and is slightly reduced as the amount of BSA in solution increases. This profile suggests a high affinity adsorption process that is partly saturated by the increasing BSA concentration. A possible explanation would be initial binding mediated by electrostatic forces, based on the opposite charge of oxidized silicon and BSA at pH 3.8. As the BSA added increases, most protein would be just adsorbed by hydrophobic interactions. BSA association at

pH 7.4, on the other hand, shows a very similar profile to that observed with insulin: a progressive AE increase at low concentrations that peaks between 1mg/mL and 3 mg/mL (~80% AE), but is reduced for very high BSA concentrations (25 mg/mL).

MS-MPs showed remarkably different LC profiles of BSA depending on the pH. At pH 7.4, MS-MPs reached maximum LC (~40%) for the maximum BSA concentration tested: 25 mg/mL. At pH 3.8, MS-MPs loading capacity reached 79% for 25 mg/mL of BSA. Such LC values imply a 4:1 BSA/silicon ratio in the formulation, a loading value hardly achieved with any other materials used in the fabrication of controlled release devices.

Figure S2 (supplementary material) shows the SEM images of protein-loaded MS-MPs. It can be seen that both insulin and BSA deposit as a uniform layer on the pore surfaces (Figure S2A and S2B, respectively). Figure S2C is a control showing the surface of unloaded MS-MPs at the same magnification. SEM images confirm that proteins are loaded on the surface of the MS-MPs, supporting our proposed loading mechanism. However, SEM images are only providing us with information about the MS-MPs outer surface, but not on any potential protein adsorbed onto the inner MS-MPs pores. Considering the amounts of protein adsorbed it is very likely that a large fraction of the proteins will be loaded in this inner structure. That is also a logical conclusion since the radius of gyration of both proteins (1.5 and 3 nm approximately for insulin and BSA, respectively) is well below the pore size of the prepared MS-MPs (34 nm).

In summary, the experimental evidence presented above confirms the excellent properties of MS-MPs as devices capable of loading therapeutic proteins. Furthermore, these experiments highlight the complexity of the adsorption process, which depends on the nature of the protein to be loaded, on the concentration of the protein solution used for adsorption, and on physicochemical parameters such as the pH. Future work will focus on studying the possibility to control protein adsorption parameters through surface modification or modulation of the carrier porosity.

Chitosan coating. Chitosan (CS) is a biodegradable, biocompatible polysaccharide with interesting features for drug delivery applications [36]. Among such features, it is worth mentioning that CS can act as a pH-sensitive controlled release polymer, that it can form polymer coatings with mucoadhesive characteristics, and that it is also a mucosal penetration enhancer. Based on these properties, we aimed at modifying the surface of MS-MPs by coating it with this polymer. To this end, modification was performed firstly in unloaded carriers and subsequently in protein-loaded ones.

Unloaded MS-MPs were used in preliminary experiments aimed to establishing the optimal pH for the CS-coating process. These studies indicated that CS does not attach to MS-MPs at strongly acidic pH values (pH 1-2), and is insoluble at neutral or basic pH. Significant CS attachment to the MS-MPs material was found in acetate buffer of pH 3.8, a buffer where CS is invariably positively charged (i.e. $pK_a \sim 6.5 - 6.8$). This could account for its adsorption onto the anionic porous silicon surface. We also observed that CS-coating in this acidic medium was time-dependent, and allowed us to form mixed silicon/CS systems where the coating polymer accounted for nearly 30% of the final formulation weight over a period of one week. However, to reduce possible MS-MPs degradation in the aqueous solvent, and potential protein release in further studies dealing with loaded particles, the CS-coating process was limited to 1 h of co-incubation. According to a previous study [13], it is estimated that only 10% or less of the MS-MPs weight could be lost under the selected experimental conditions.

Once established the optimal coating method, we investigated the effect of CS chemical properties (molecular weight, degree of acetylation) and CS concentration in the efficiency of CS incorporation into the final system. CS-coating efficiency was measured by quantifying CS through a colorimetric method. Table 1 summarizes the CS coating efficiencies achieved. This parameter measures the percentage of the original CS mass that is incorporated into the formulation during the coating procedure. In general, all CS samples exhibited low affinities for the MS-MPs, with CS-coating efficiencies below 4%. As we have mentioned, efficient CS absorption required rather long incubation times, suggesting that longer times might be beneficial to induce some cooperative binding of CS.

Additionally, CS has large gyration radius (37-96 nm; F.M. Goycoolea, unpublished work) as compared to the average pore size of MS-MPs (~35 nm). Hence, CS penetration to the inner structure would be sterically hindered, resulting on specific CS deposition on the external shell of the MS-MPs. The external surface of the MS-MPs is several orders of magnitude lower than the total surface of the system, and this might be an important reason for the moderate fractions of CS bound. This hindered penetration of CS, however, could be considered advantageous since it allows depositing a CS coating layer without interfering in the inner carrier structure.

From our experiments with different CS samples, we can draw the following general rules regarding their capacity to coat MS-MPs. Firstly, CS with low degrees of acetylation are more efficient for coating than samples of CS with high degree of acetylation (Table 1). These differences exceeded one order of magnitude when comparing samples of similar degree of polymerization. CS with high degree of acetylation have low molar fractions of D-glucosamine residues that are susceptible to become protonated at pH 3.8, which in turn, should induce a small positive charge on the polymeric chain and ultimately a low binding to the oxidized silicon matrix. This is consistent with the view that the interaction between MS-MPs and CS is mainly mediated by electrostatic forces rather than by hydrophobic interactions. Secondly, experiments performed with CS samples with degree of acetylation of 1% but different degrees of polymerization revealed that more efficient coating is achieved with the largest CS molecules. Indeed, MS-MPs associated about 3-fold more CS of high degree of polymerization (HDP-DA1) than CS of low degree of polymerization (LDP-DA1). A possible explanation is that the increase in Mw results in a reduction in cooperative length of CS that effectively interacts with the MS-MP surface. In a recent work that has addressed the interaction between CS and the surface of dipalmitoyl-sn-glycero-3-phosphocholine (DPPC) bilayers, it has been observed that the increase of CS Mw leads to a dramatic reduction in the cooperative unit and hence an increase in effective contact area between individual CS and the lipid bilayer [37]. This reduction in the cooperative effective length against Mw implies that CS swirls across the surface bilayer, thus forming ‘trains’ [38].

A similar mechanism may operate for the interaction between CS and MS-MP surface. Based on these results we decided to use HDP-DA1 CS and fix its concentration in the coating solutions to 0.7 mg/mL, the concentration that rendered the most efficient process.

On protein-loaded MS-MPs we initially aimed at confirming that the coating process would not induce the release of significant amounts of the loaded proteins. Our experiments confirmed that BSA release during CS-coating is negligible, while it amounts to less than 20% in the case of insulin-loaded materials.

Figure 5 illustrates the change in microparticle composition as a function of the amount of loaded BSA. The percentage of CS in the coated formulation increases with BSA loading, achieving a maximum CS-incorporation for an MS-MPs:BSA mass ratio of 1. Similar results were obtained with insulin-loaded MS-MPs (results not shown).

AFM was used to visualize the surface topology of CS-coated MS-MPs at nanometric resolution (Figure S3). These images corroborate that after CS-coating the external surface of the MS-MPs becomes rougher (Figure S3A and S3B). Indeed, the presence of globular structures in the systems coated with CS can be attributed to the formation of an irregular film of the polymer around the solid silicon matrix. Similar surface topologies were found with protein-loaded CS-coated MS-MPs (Figure S3C).

Altogether, these results indicate the success of our coating optimized protocol. CS mass percentages around 2-4% in the formulation might seem insufficient for preparing useful coatings. However, it should be considered that MS-MPs are 33 μm in size, and thus, this system presents a moderate specific surface for molecules with restricted access to the mesopores. For such systems, relatively small amounts of coating polymers are necessary for surface modification.

In Vitro Release. In vitro tests were conducted to study insulin release from MS-MPs at two different pH values (7.4 and 5.5), and under sink conditions. Experiments were performed both for uncoated and CS-coated MS-MPs and the results are presented in Figure 6. At pH 5.5 both uncoated and CS-coated

MS-MPs showed similar (probably due to the chitosan swell) biphasic release profiles: an initial burst of 30-35%, a slow release of another 10% of the cargo up to 45 minutes, and then a fast release of the protein (30-40% of the cargo) in the next 15 minutes. At pH 7.4, both uncoated and CS-coated formulations showed a more progressive release profile. In uncoated MS-MPs, insulin burst release was restricted to 20% of the payload, and 60% of the loaded peptide was released by the 45 min time point. For CS-coated MS-MPs, a slower release profile was detected: burst release was also restricted to 20% of the total insulin, while further 40% was released by the 45 min time point. In this particular case, 90% insulin release was reached approximately after 90 min.

Both MS-MPs show fast, but controlled release of insulin, as illustrated by the low burst effect and the capacity of the formulation to maintain insulin release for more than 1 h. This contrasts with more uncontrolled profiles typical from some other CS-based delivery devices such as CS nanoparticles [38]. Considering that MS-MPs are not expected to degrade in such short time spans, and the progressive release kinetics observed for CS-coated MS-MPs at pH 7.4, we believe that insulin release from MS-MPs must be diffusion-controlled. This diffusion-controlled kinetic would be related both to insulin transport through the nanometric pores, and to insulin transport through the CS-coating. Interestingly, our insulin release profile is very similar to that reported very recently by Wu et al. using SiO₂ films covalently attached to CS [24]. However, MS-MPs might present two technical advantages for drug delivery: (1) MS-MPs are in a particulated form that can be easily administered by mucosal routes or even implanted by injection; (2) CS-coated MS-MPs undergo a coating procedure based on electrostatic interactions between CS and the MS-MPs that does not involve covalent attachment. The fact that similar insulin release profiles can be obtained with CS-coated MS-MPs and CS-coated SiO₂ suggests that our optimized electrostatic-based coating procedure provides similar benefits to CS-covalent linking, but would not generate any further regulatory concern related to the formation of a new chemical entity.

In summary, MS-MPs and CS-coated MS-MPs release profiles might be particularly adequate for the applications where fast but not instantaneous release of insulin is desired, for instance, in many mucosal delivery applications. Considering our experience with MS-MPs and CS, we believe that other more prolonged release profiles should be possible for other applications, by modulating MS-MPs inner structured and the coating polymer.

Conclusions

A new promising composite device for protein and peptide controlled delivery has been designed. This device is based on mesoporous silicon materials prepared by a new electrochemical method and dispersed in the form of microparticles (MS-MPs). These microparticles can be optionally coated with the polysaccharide CS for the modification of its in vitro release profile, and potentially, to integrate other desirable features in the device (mucoadhesion, permeation enhancing properties). MS-MPs present an outstanding capacity to load proteins by adsorption, with adequate association efficiencies and remarkably high loadings. Indeed, with this mesoporous systems it is possible to prepare formulations where the loaded protein mass is higher than the mass of the carrier itself. Studies of insulin release from the MS-MPs indicated that release from the prepared devices is very fast (>80% insulin released at 45 min) but controlled (burst release below 20%). Modification of MS-MPs through a CS-coating slows down insulin release to a certain extent. Overall, the characteristics of these drug delivery devices indicate its potential interest for formulating labile biopharmaceuticals, and particularly as transmucosal delivery devices.

Acknowledgements

EP and EM acknowledge financial support of IMPIVA (IMIDTP/2009/152) and MICINN (PTQ-09-01-00836). MGF acknowledges an Isidro Parga Pondal contract from Xunta de Galicia. FMG

acknowledges a Fellowship from the FP7-Marie Curie Program. This work was financed by Consellería de Innovación e Industria, Xunta de Galicia (PGIDIT07PXIB203067PR) and the Spanish Ministry of Science and Innovation (Programa de Investigación en Salud, PS09/01786).

References

- [1] W. Sun, J.E. Puzas, T.J. Sheu and P.M. Fauchet, *Phys. Stat. Sol. (A)*, 204, 5 (2007) 1429.
- [2] A. Ressine, G Marko-Varga and T. Laurell, *Biotechnol Annu Rev.*, 13 (2007) 149.
- [3] C.A. Prestidge, T.J. Barnes, A. Mierczynska-Vasilev, W. Skinner, F. Peddie and C. Barnett, *Phys. Stat. Sol. (A)* 204 (2007) 3361.
- [4] E. Pastor, M. Balaguer, L. Bychto, J. Salonen, V.-P. Lehto, E. Matveeva and V. Chirvony, *J. Nanosci. Nanotechnol.* 9, 6 (2009) 3455.
- [5] L.T. Canham, A. Nassiopoulou, V. Parkhutik, M. Sailor and E. Matveeva (Eds.), *Extended Abstracts Porous Semiconductors Science and Technology (IV)*. Valencia, March 15-19, 2004, p. 102.
- [6] L. Vaccari, D. Canton, N. Zaffaroni, R. Villa, M. Tormen and E. Fabrizio, *Eng.*, 83 (2006) 1598.
- [7] E.J. Anglin, M.P. Schwartz, V.P. Ng, L.A. Perelman and M.J.Sailor, *Langmuir*, 20 (2004) 11264.
- [8] V. Chirvony, V. Bolotin, E. Matveeva and V. Parkhutik, *J. Photochem. Photobiol. A—Chem.*, 181 (2006) 106.
- [9] S.C. Bayliss, R. Heald, D.I. Fletcher and L.D. Buckberry, *Adv. Mater.*, 11 (1999) 318.
- [10] L. Bimbo, M. Sarparanta, H. Santos, A. Airaksinen, E. Makila, T. Laaksonen, L. Peltonen, V.-P. Lehto, J. Hirvonen and J. Salonen, *ACS Nano*, 4 (2010) 3023.
- [11] L.T. Canham, *Adv. Mater.*, 7 (1995) 1033.
- [12] E.J. Anglin, C. Lingyun, W.R. Freeman and M.J. Sailor, *Adv. Drug Deliv. Rev.*, 60 (2008) 1266.
- [13] J. Salonen, A.M. Kaukonen, J. Hirvonen and V.-P. Lehto, *J. Pharma. Sci.* 97, 2 (2008) 632.

- [14] F. Martina, R. Walczaka, A. Boiarskia, M Cohena, T. Westa, C. Cosentino, and M. Ferrari, J. Control Release, 102 (2005) 123.
- [15] LT Canham, A Nassiopoulou, V Parkhutik, M Sailor and E Matveeva (Eds.), Extended Abstracts Porous Semiconductors Science and Technology (V), Barcelona, March 12-17, 2006. p. 422.
- [16] S.L. Tao and T.A Desai, Drug Discovery Today, 10 (2005) 909.
- [17] A.B. Foraker, R.J. Walczak, M.H.Cohen, A.A. Boiarski, C.F. Grove and P.W. Swaan, Pharm. Res., 20 (2003) 110.
- [18] C.A. Prestidge, T.J. Barnes, A. Mierczynska-Vasilev, I. Kempson, F. Peddie and C. Barnett, Phys. Stat. Sol. (A), 205 (2008) 311.
- [19] C.A. Prestidge, T.J. Barnes, A. Mierczynska-Vasilev, W. Skinner, F. Peddie and C. Barnett, Phys. Stat. Sol. (A), 204 (2007) 3361.
- [20] L.M. Karlsson, P. Tengvall, I. Lundstrom, and H. Arwin, Phys. Stat. Sol. (A) 197 (2003) 326.
- [21] L.M. Karlsson, P. Tengvall, I. Lundstrom, and H. Arwin, J. Colloid Interface Sci., 266 (2003) 40.
- [22] C.A. Prestidge, T.J. Barnes, C.H. Lau, C. Barnett, A. Loni and L. Canham, Expert Opinion on Drug Delivery, 4 (2007) 101.
- [23] E. Tasciotti, X. Liu, R. Bhavane, K. Plant, A.D. Leonard, B.K. Price, M. Cheng, P. Decuzzi, J.M. Tour, F. Robertson and M Ferrari, Nature Nanotechnology, 3 (2008) 151.
- [24] J. Wu and M.J. Sailor, Adv. Funct. Mater., 19 (2009) 733.
- [25] F. Cui, F. Qian, Z. Zhao, L. Yin, C. Tang, C. Yin, Biomacromolecules, 10, (2009) 1253.
- [26] P. Calvo, C. Remuñán-Lopez, J.L. Vila-Jato and M.J. Alonso, J. Appl. Polym. Sci., 63 (1997) 125.

- [27] J.H. Hamman, M. Stander and A.F. Kotzé, *Int. J. Pharm.*, 232 (2002) 235.
- [28] P. Sorlier, A. Denuziere, C. Viton and A. Domard, *Biomacromolecules*, 3 (2001) 765.
- [29] S. Fienel, K.M. Vårum, M.M. Fiumnu, A.A. Hincal (Eds.), 9th International Conferences of the European Chitin Society. Antalya, 8-11 Sept. 2007, p. 542.
- [30] R.A.A. Muzzarelli, *Analytical Biochemistry*, 260 (1998) 255.
- [31] K.L. Jarvis, T.J. Barnes and C.A. Prestidge, *Langmuir*, 24 (2008) 14222.
- [32] E. Pastor, E. Matveeva, V. Parkhutik, J. Curiel-Esparza and M.C Millan, *Phys. Status Solidi (C)*, 4 (2007) 2136.
- [33] K.L. Jarvis, T.J. Barnes and C.A. Prestidge, *Langmuir*, 26 (2010) 14316.
- [34] Bisi O., Ossicini S. and Pavesi L., *Surface Science Reports*, 38, 1 (2000) , 1-126.
- [35] C. Ortiz, D. Zhang, Y. Xie, V.J. Davisson and D. Ben-Amotz, *Anal. Biochemical*, 332 (2004) 245.
- [36] S.A. Agnihotri, N.N. Mallikarjuna and T.M. Aminabhavi, *J. Control Release*, 100 (2004) 5.
- [37] N. Fang, V. Chan, H.Q. Mao and K.W. Leong, *Biomacromolecules*, 2 (2001) 1161.
- [38] Y.H. Chang, Y.D. Lee, O.J. Karlsson and D.C. Sundberg, *Polymer*, 41 (2000) 6741.
- [39] R. Fernández-Urrusuno, P. Calvo, C. Remuñán-López, J.L. Vila-Jato and M.J Alonso, *Pharm. Res.*, 16 (1999) 1576.

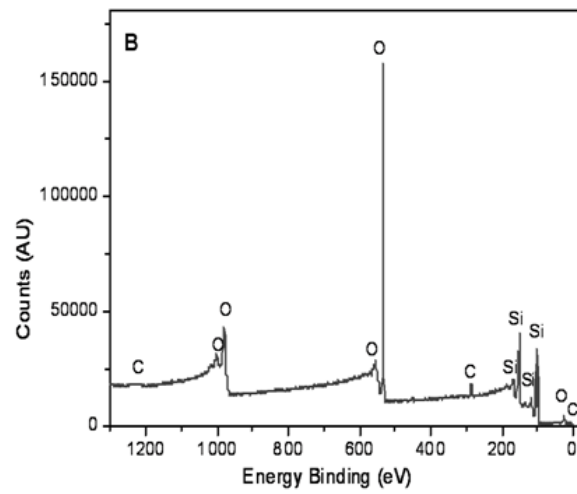
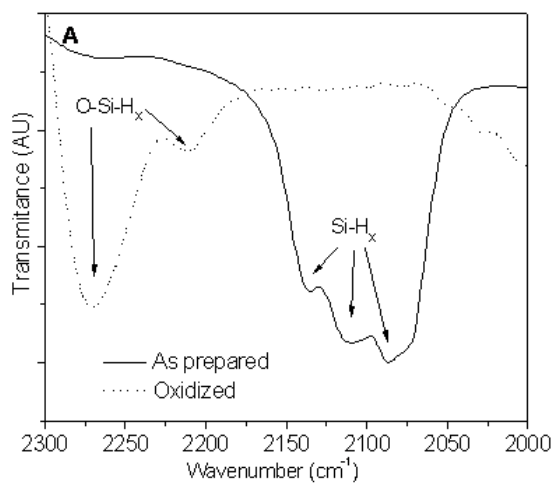


Figure 1

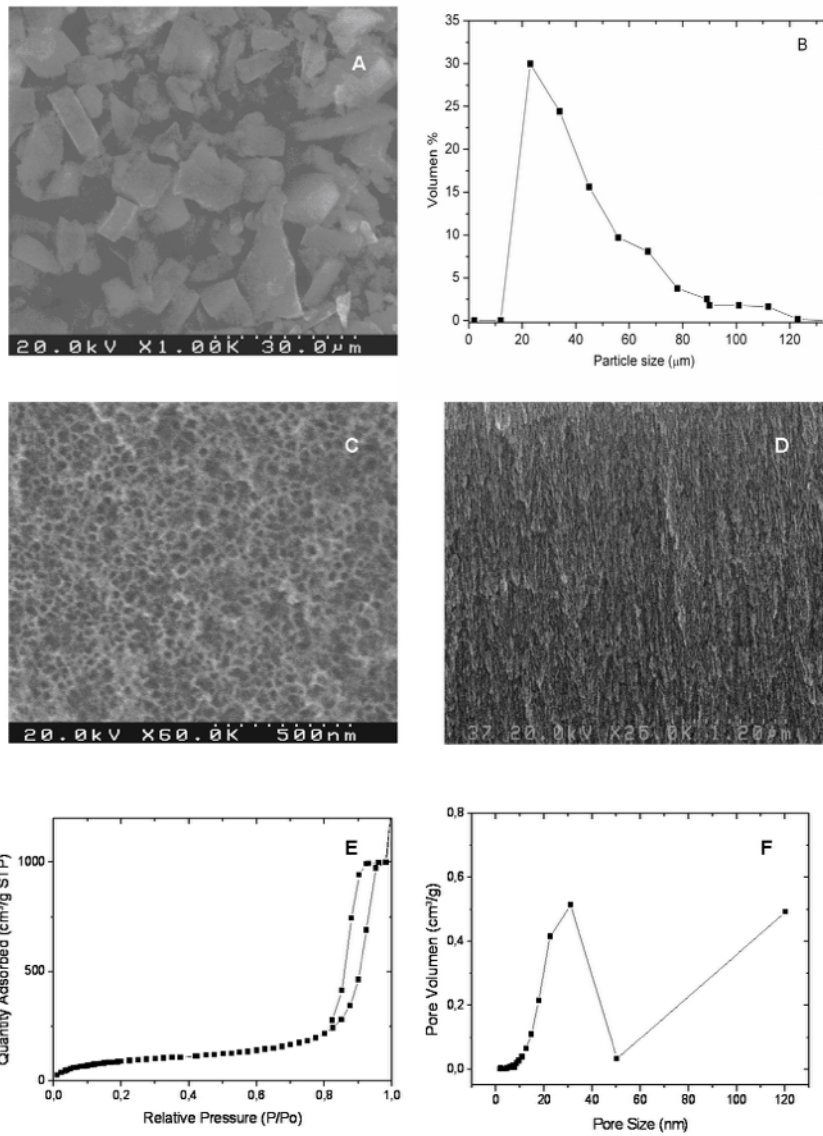


Figure 2

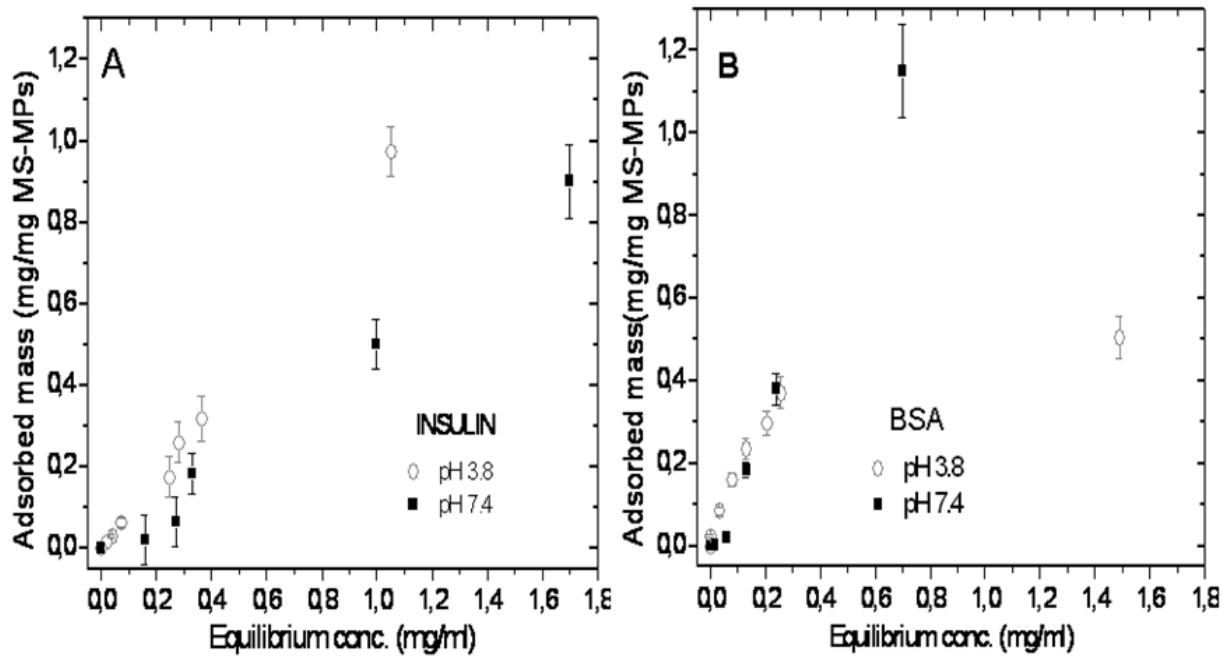


Figure 3

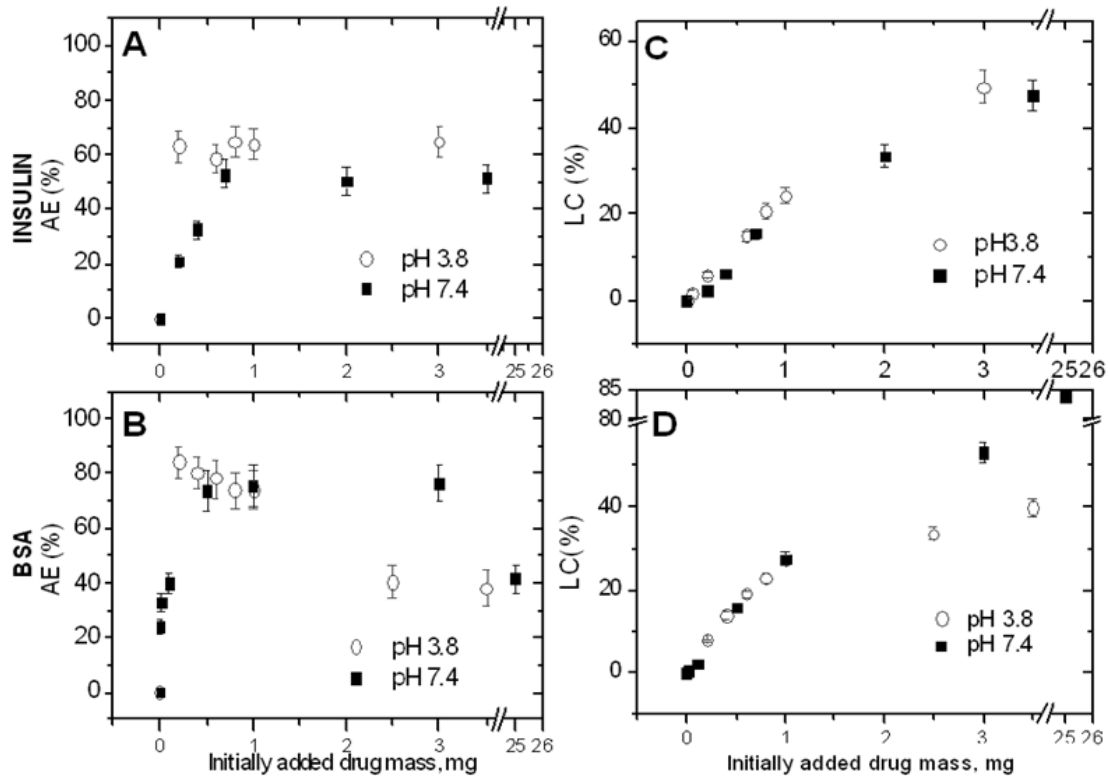


Figure 4

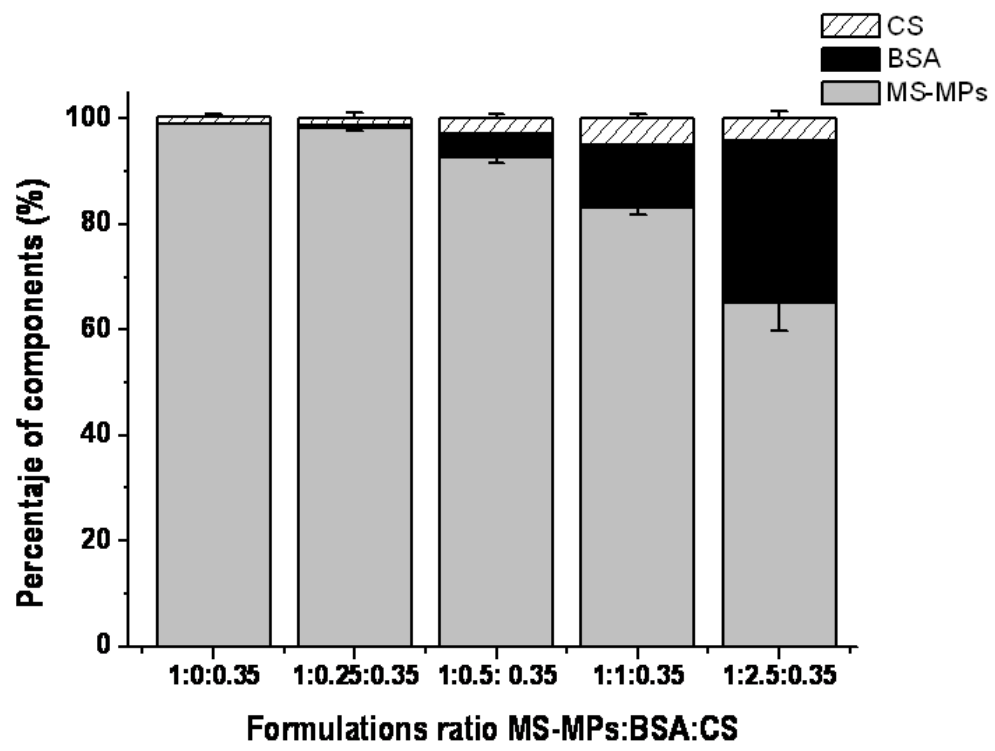
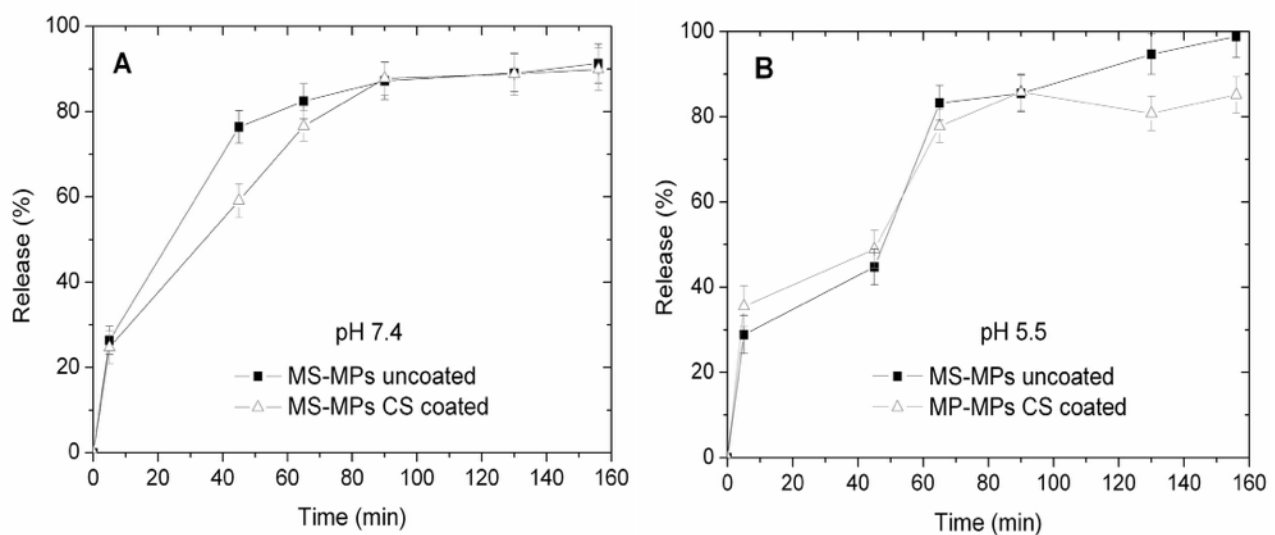


Figure 5

Figure 6



Supplementary material

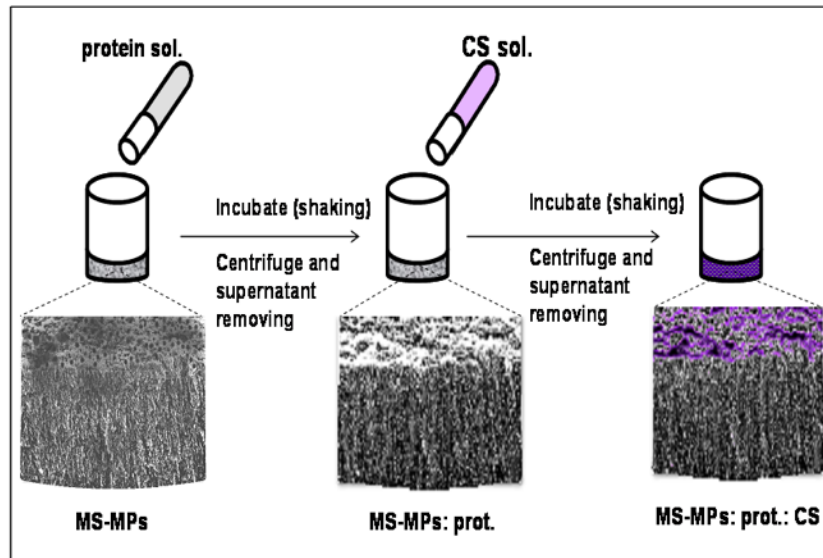


Figure S1. Scheme of the different steps taken for the preparation of the drug delivery device. The upper figure shows loading of protein at the first step and coating by CS in the second step. The lower figure shows a schematic representation of the expected microstructure of the material at each step.

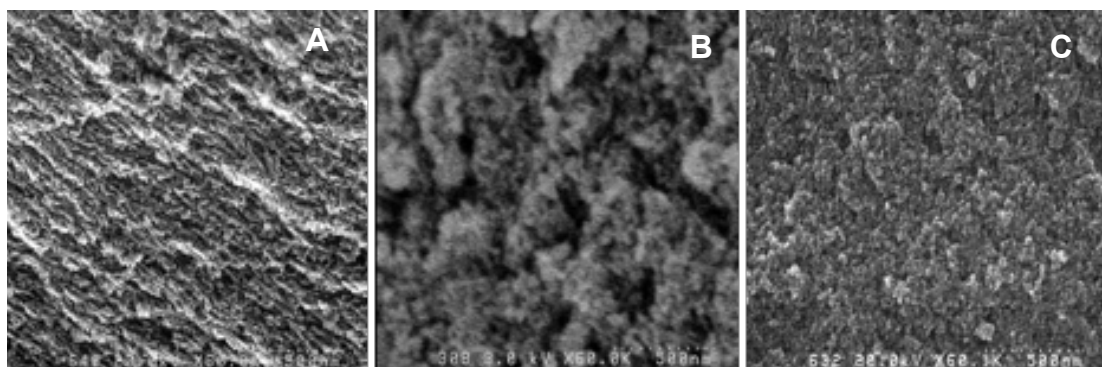


Figure S2. SEM images of insulin- and BSA-loaded mesoporous silicon microparticles. (A) Insulin loaded. (B) BSA loaded, (C) unloaded control. All micrographs were taken at the same magnification.